Melt Spun Microporous Fibers Using Poly(lactic acid) and Sulfonated Copolyester Blends for Tissue Engineering Applications

Ruwan D. Sumanasinghe,[1,2] Carla M. Haslauer,[1] Behnam Pourdeyhimi,[1,2] Elizabeth G. Loboa[1]

[1]*Joint Department of Biomedical Engineering, University of North Carolina at Chapel Hill and North Carolina State University, Raleigh, North Carolina*
[2]*College of Textiles, North Carolina State University, Raleigh, North Carolina*

Received 13 August 2008; accepted 27 December 2009
DOI 10.1002/app.32025
Published online 11 May 2010 in Wiley InterScience (www.interscience.wiley.com).

ABSTRACT: Microporous fibers can potentially increase diffusional properties of three-dimensional nonwoven scaffolds used for tissue engineering applications. We have investigated the use of a water-dispersible copolyester, sulfonated copolyester (SP), to create micropores in composite fibers containing a blend of SP and poly(lactic acid) (PLA) at 1, 3, 5, and 10% SP content. PLA and SP were blended at 175°C in a microcompounder followed by extrusion of composite fibers and removal of SP from composite fibers by using hydrodispersion to form micropores in the composite fibers. Differential scanning calorimetric studies on unhydrolysed composite fibers showed that SP was partially miscible in PLA. Fourier transform infrared mapping of composite fiber cross sections revealed that SP was randomly dispersed throughout the cross section where the degree of dispersion depended on the SP content. As revealed by the scanning electron micrographs, the size of the micropores was dependent on the SP content. Micropores on fiber cross sections were observed in fibers above 3% SP indicating that at least 3% SP content is needed to produce droplet morphology of SP in these fibers. These results show that SP can be successfully used in a blend with PLA to produce microporous fibers to fabricate three-dimensional nonwoven scaffolds for tissue engineering applications. © 2010 Wiley Periodicals, Inc. J Appl Polym Sci 117: 3350–3361, 2010

Key words: biomaterials; blends; fibers; water soluble polymers

INTRODUCTION

Apart from biocompatibility, bioresorption, and mechanical stability, three-dimensional scaffolds for tissue engineering applications require increased diffusional properties to allow flow of culture media or blood throughout the scaffold leading to uniform cell growth *in vitro* and *in vivo*.[1,2] Scaffolds fabricated using polymeric fibers provide the advantage of being able to engineer properties such as strength, pore size, porosity, and rate of bioresorption.[3] However, increased thickness of three-dimensional scaffolds is limited by decreased diffusion to the center of the scaffolds. Successful development of three-dimensional substrates for tissue engineering applications will be governed by the availability of scaffolds with greater diffusion properties.

Nonwoven structures with their inherent porosity and (somewhat) random fiber arrangement can be manipulated to mimic the extracellular matrix of a tissue and thus are regarded as a suitable source for tissue engineering scaffolds. Although nonwoven structures possess fiber interstices and pores that could create channels for media or blood flow, increases in thickness of these structures could create barriers to flow in the transverse direction. Replacement of solid fibers with microporous hollow fibers or fibers consisting of microchannels in nonwoven scaffolds are greatly expected to enhance their diffusional properties. Hollow fibers can be spun by using existing fiber technology. However, creation of micropores on fiber surfaces or microchannels in fibers poses a challenge that needs to be addressed.

Previous studies have shown that polyester can be physically modified to create pores by adding 0.2–2% of dry process silica with an average primary particle size of 0.1 μm[4] or 0.4–5% of colloidal $CaCO_3$ with a size of 0.02–0.3 μm[4] or 0.5–5% of kaolinite.[4] In addition, chemical substances such as 3% Na alkanesulfonate, 1% Na magnesium dicarboxybenzene-sulfonate and a 1.2% mixture of polyethylene glycol and C12–13 alkanesulfonic acid sodium salt added to polyester result in better pore formation during treatment with alkali after spinning. In the case of polyolefins, the crystallization characteristics of the polymer alone can be utilized to form micropores. Micropores that extend from the surface to the interior of the fiber can be created using a combination of heat and draw steps during spinning of

Correspondence to: E. G. Loboa (egloboa@ncsu.edu).
Contract grant sponsor: Nonwovens Cooperative Research Center at North Carolina State University.

polyolefins.[4] Fatty acid systems, such as oleic acid, linoleic acid, or soybean mixtures have been added as diluents to polypropylene (PP). By controlling the temperature of the coagulation bath, a thermally induced phase separation takes place and the mobility of the diluent determines the size of the micropores within the PP spherulite.[5] The use of liquid paraffin and polybutene as diluent agents in PP has been explored.[4] Similar to PP, it is possible to process polyethylene (PE) with diluents as plasticized melt. Mixtures of high density polyethylene (HDPE) with 2-butoxyethyl oleate, BU stearate or bis(2-ethylehexyl) phthalate can be spun into hollow fibers and made microporous by cooling with isopropanol and leaching in ethanol.[4] However to date, the use of a hydrolysable or water-dispersible polymer blended with a more stable polymer to create micropores in the fibers have not been fully investigated.

The purpose of this study was to investigate the use of a water-dispersible polymer, sulfonated copolyester (SP) as a minor phase dispersed in a poly(lactic acid) (PLA) matrix, to create micropores in PLA/SP composite fibers. A compounder was used to blend PLA with SP at different proportions in the molten state and melt extrude fibers. The resultant fibers were analyzed for their thermal properties and localization of SP in composite fibers. The SP was removed from the composite fibers by hydrodispersion and the resultant fibers were microscopically analyzed for the presence of pores.

MATERIALS AND METHODS

Preparation of polymers

Poly(L-lactic acid)[6] (PLA; Viscosity average molecular weight = 70,333) (Nonwovens Corporative Research Center, North Carolina State University, Raleigh, NC) in granule form and water-dispersible SP (Weight average molecular weight = 20,000) also known as EastONE (Eastman Chemical Company, Kingsport, TN) in flake form were stored in desiccators and vacuum dried before use. The structures of PLA and SP are illustrated by a and b.

PLA

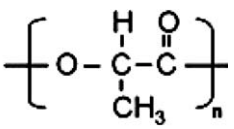

(a)

SP HO-G-A-G-A-[G-A]$_4$-G-A-G-A-G-OH

($SO_3^-Na^+$ groups on the A units)

G - aliphatic/cycloaliphatic glycol moiety
A - aromatic dicarboxylic acid moiety

(b)

Filament extrusion

Blending of PLA and SP was carried out in their molten state. Briefly, PLA was ground to particle form and physically mixed with varying proportions of SP to obtain 99%PLA/1%SP, 97%PLA/3%SP, 95%PLA/5%SP, and 90%PLA/10%SP polymer mixtures. The filaments from each polymer mix were extruded using a HAAKE MiniLab micro compounder (Thermo Electron, Newington, NH) fixed with counter rotating conical twin screws with nitrogen as inert gas. The polymer mix was heated at 175°C with a 10–15 min recirculation (residence) time in the microcompounder before extruding through a 0.5 mm orifice fitted externally to the body of the compounder. In addition to the above polymer blends, 100% PLA and 100% SP filaments were extruded and used as controls. The spinning was followed by hot drawing at a constant draw ratio.

Water dispersion of sulfonated polyester from composite fibers

The resultant fibers of 99%PLA/1%SP, 97%PLA/3%SP, 95%PLA/5%SP, and 90%PLA/10%SP were then hydrodispersed for two hours in 50 mL of deionized water using an orbital reciprocating water bath (Boekel Scientific, Feasterville, PA) at 70°C and 140 rpm and subsequently in an ultrasonicator (Cole-Parmer Instrument Company, Chicago, IL) at 70°C. Fibers were then dried in a vacuum oven for 24 h at 55°C.

Characterization of single component and composite fibers

Differential scanning calorimetry

Thermal properties of the PLA, SP polymers, and PLA/SP composite fibers were measured by differential scanning calorimetry (DSC) using a Perkin-Elmer Diamond DSC (PerkinElmer Life and Analytical Sciences, Shelton, CT) equipped with Pyris software (V5.0). Approximately 3–5 mg of PLA and SP polymer samples were heated from room temperature to 200°C at 20°C/min, held for 4 min at 200°C and then cooled from 200 to 25°C at 20°C/min to obtain the glass transition temperature and melt peak temperature for each specimen. The degree of crystallinity was calculated using eq. 1.1.[7] Three DSC scans were run for each sample to calculate average and standard deviation of each parameter.

$$\text{Degree of Crystallinty} = \frac{\Delta H_m - \Delta H_C}{\Delta H_{m(100\%)}} \qquad (1.1)$$

where, $\Delta H_{m(100\%)}$ = 93.6 J/g for 100% crystalline PLA,[8,9] ΔH_m = Measured enthalpy of melting; ΔH_c = Measured enthalpy of crystallization.

Minor phase morphology

Morphology of the SP minor phase in PLA/SP fiber blend was studied by analyzing the melt viscosity data acquired from the mini compounder. The viscosities of both 100% PLA and 100% SP were used to calculate the viscosity ratio, i.e. the viscosity of the dispersed phase (SP)/the viscosity of the matrix (PLA). These ratios were plotted against time to determine the behavior of minor phase (SP) in the PLA matrix during resident (blending) time in the microcompounder.

Preparation of composite fiber cross sections

Three fiber samples having an approximate length of 2 inches were cut randomly along the length of each extruded composite filament. The fibers from each composite filament were placed in a polyethyelene capsule and embedded in a resin using the PELCO® Eponate 12T embedding kit (Ted Pella, Redding, CA). The resin embedded fiber cross sections with thicknesses of 20 and 40 μm were cut using a microtome (Reichert Microscope Services, Depew, NY).

Microscopic analysis and pore size measurement

To ascertain the extent of hydrolysis and micropores on the fiber surface and throughout fiber cross sections, the surfaces of the hydrolysed and unhydrolysed composite fibers and their 40 μm cross sections were viewed under a scanning electron microscope (SEM). The fibers and fiber cross sections were mounted on aluminum stubs using conductive self-adhesive tape (Ted Pella, Redding, CA) and coated with gold/palladium (thickness of 20 nm) using a HUMMER 6.2 sputter coater (ANATECH Ltd, Springfield VA). Images of the coated samples were acquired from a JEOL JSM 5900 Scanning Electron Microscope (JEOL USA, Peabody, MA) using an accelerating voltage of 15 kV and a spot size of 15 nm. Multiple random micrographs of fiber cross sections were obtained at 1000× and 2500× while fiber surfaces were micrographed at 2500×. The size of pores on the hydrolysed fiber surfaces were measured using scanning electron micrographs (2500×) and SimplePCI image analysis software (Compix, Image Systems, Cranberry Township, PA). Each area analyzed under 2500× amounted to 0.02 mm^2 area of the fiber surface. The number of pores per mm^2 area of the fiber surface was presented as a frequency distribution.

Localization of SP by using Fourier transform infrared spectroscopy

Both 100% PLA and 100% SP polymers were scanned using a Fourier Transform Infrared (FTIR)-Spectrophotometer (Nicolet Model 510P) fitted with an attenuated total reflectance (ATR) attachment and a DTGS detector. A total of 64 scans were aggregated between 600 and 3000 cm^{-1} with each spectrum at 2 cm^{-1} resolution. The bands in the spectra were analyzed using OMNIC v7.2 software. The FTIR band at 1717.7 cm^{-1}, which corresponds to C=O stretching[10] in 100% SP polymer was used to detect the localization of SP polymer in composite fiber cross sections.

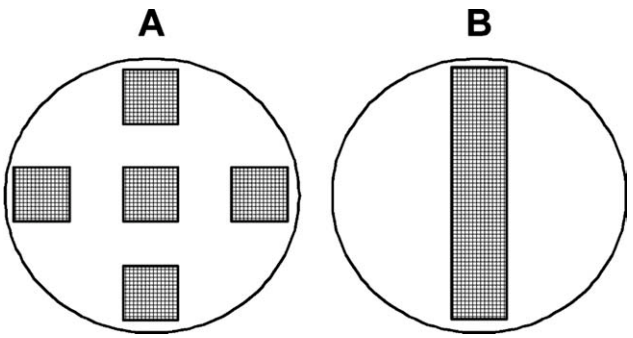

Figure 1 Arrangement of area maps on 20 μm thick unhydrolysed composite fiber cross sections for analysis using the mapping function of the Fourier transform infrared spectrophotometer. (A) Arrangement of maps for the first fiber cross section, and (B) Arrangement of the map for second and third fiber cross sections of the same fiber.

To detect localization of SP in composite fiber cross sections, the 20 μm thick composite fiber cross sections were mapped using a FTIR (Thermo Nicolet Nexus 470) fitted with a Continuμm microscope and a Mercury Cadmium Telluride (MCT) detector at 150×. A map of the area to be scanned on each fiber cross section was created using Atlμs v7.7 mapping software. Three fiber cross sections of unhydrolysed 99% PLA/1% SP, and 90% PLA/10% SP fibers were mapped using two different mapping configurations (Fig. 1). Cross sections from each type of fiber were mapped at center, right, left, top, and bottom using an area map having a total area of 12.1×10^3 μm^2 (0.012 mm^2) per location. Two more cross sections from the same type of fiber were mapped across the fiber diameter using an area map having 50 μm width and length based on the diameter of the fiber. A total of 64 scans in reflectance mode were aggregated between 600 and 3000 cm^{-1} with each spectrum at 2 cm^{-1} resolution. The band at 1717.7 cm^{-1} was selected in the acquired spectra of unhydrolysed composite fiber samples to identify the localization of SP in composite fiber cross sections. The specific localization of SP was presented in the form of contour (2D) and 3D area maps showing location and intensity of the bands.

RESULTS

Differential scanning calorimetry

The thermograms of PLA exhibited a glass transition at 61.93°C with a crystallinity of 36.04 ± 1.28%

TABLE I
Thermal Properties of PLA and SP Using Differential Scanning Calorimetry

Polymer	Glass transition temperature (°C)	Crystallinity (%)
PLA	62 ± 5	36 ± 1
SP	56 ± 1	None

(Table I). In contrast, all SP polymer samples examined had glass transitions at 55.77°C (Table I) without a melt peak indicating that SP was an amorphous polymer. All unhydrolysed composite fibers and 100% PLA showed a glass transition temperature around 55°C (Table II) while glass transition temperatures of unhydrolysed 100% SP fibers were lower (Table II). A secondary glass transition in addition to the main glass transition was observed in 10% SP/90% PLA composite fibers (Fig. 2). The melt endotherm of all fibers consisted of a split peak (not shown). The percent crystallinity calculations revealed that the extruded 100% PLA and composite fibers were amorphous (Table II).

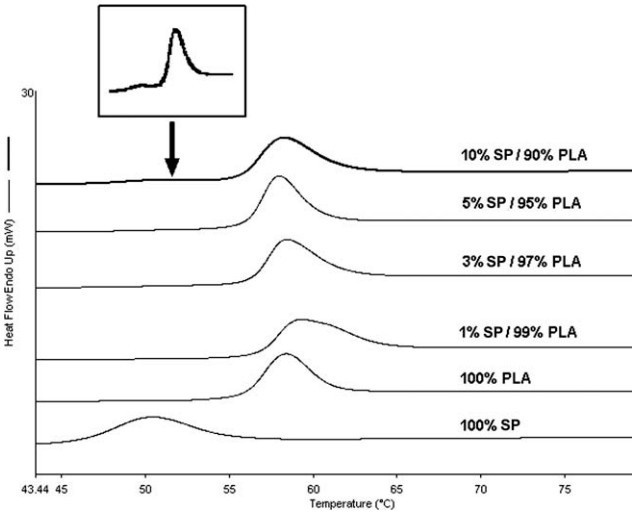

Figure 2 Glass transitions of unhydrolysed pure and composite fibers. Inset: Indicates a secondary glass transition in 90% PLA/10% SP composite fibers.

Analysis of composite fibers

Minor phase morphology in PLA/SP blend

The morphology of the minor phase achieved during melt mixing of PLA/SP would determine the size and distribution of pores in the resultant fibers. The change in viscosity and torque ratio during melt mixing can be used to predict the final morphology of the minor phase in the PLA/SP blend. The initial melt viscosity of both pure polymers and PLA/SP polymer blends [Fig. 3(A)] decreased during mixing. A change in melt viscosities of 99% PLA/1% SP is shown as a representative sample in Figure 3(A). The melt viscosity of both polymers observed after 2 min of residence time in the mini compounder showed that 100% PLA had a higher melt viscosity than that of 100% SP. A lower viscosity of SP compared to PLA ensured that SP minor phase could be finely and uniformly distributed in PLA major component. The calculated torque ratio (torque of the dispersed phase/torque of the matrix) by using torques of 100% PLA and 100% SP remained below 1 during the mixing period indicating that SP minor phase was evenly distributed in PLA matrix [Fig. 3(B)].

TABLE II
Thermal Properties of Unhydrolysed Pure and Composite Fibers

Polymer	Glass transition temperature (°C)	Crystallinity (%)
100% SP	43.88 ± 0.94	Amorphous
100% PLA	55.55 ± 0.25	Amorphous
99% PLA/1% SP	56.23 ± 0.52	0.30 ± 0.23
97% PLA/3% SP	55.43 ± 0.53	Amorphous
95% PLA/5% SP	55.50 ± 0.09	Amorphous

Microscopic analysis and pore size measurement

The micropores on composite fiber surfaces caused by hydrolysis of SP were visible in all combinations of composite fibers (Fig. 4). The pores were randomly distributed over the fiber surface irrespective of the percentage of SP in composite fibers. Scanning electron micrographs of these pores obtained at higher magnification showed that pores continued into the body of the fiber (Fig. 5). Although micropores were not observed in 99% PLA/1% SP fiber cross sections [Fig. 6(A,B)], fibers with 3%, 5% (not shown), and 10% SP [Fig. 6(C,D)] showed randomly distributed pores in their cross sections. The majority of the pores on composite fibers with less than 10% SP were below 1 μm^2 while composite fibers with 10% SP had a significant number of pores greater than 1 μm^2 (Fig. 7).

Localization of sulfonated copolyester using Fourier transform infrared spectroscopy (FTIR)

The FTIR spectra of 100% PLA polymer had bands typically observed in PLA. The spectra consisted of an aliphatic C—H stretching region between 3000 and 2850 cm^{-1} (not shown), a C=O stretching band at 1752 cm^{-1} and asymmetric stretching vibrations of C—C(=O)—O and O—C—C between 1300 cm^{-1} and 1100 cm^{-1} [Fig. 8(B)].[10] In addition, bands characteristic to PLA were also observed at 1268, 1183, 1129, 1086, and 1046 cm^{-1}.[10] FTIR spectra of 100% SP polymer consisted of a C=O stretching band at

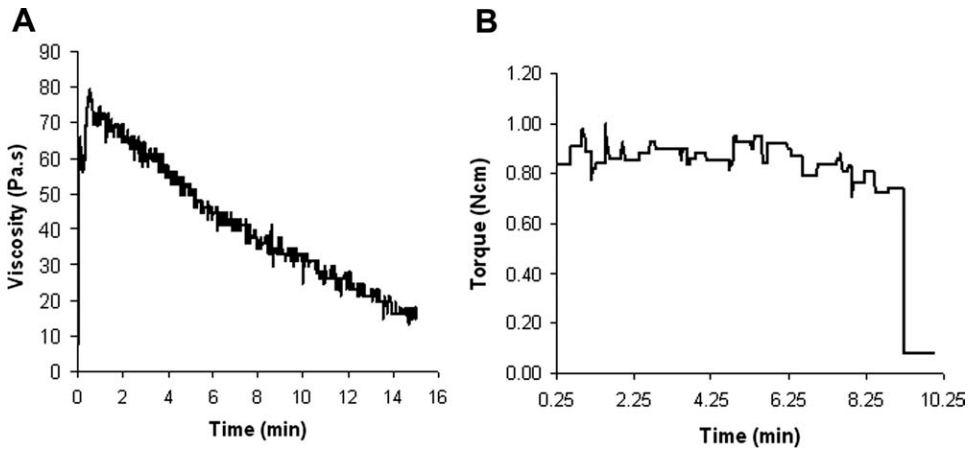

Figure 3 Melt behavior of SP and PLA showing (A) Change in melt viscosity of 99% PLA/1% SP during mixing, and (B) Change in torque ratio of 100% PLA and 100% SP.

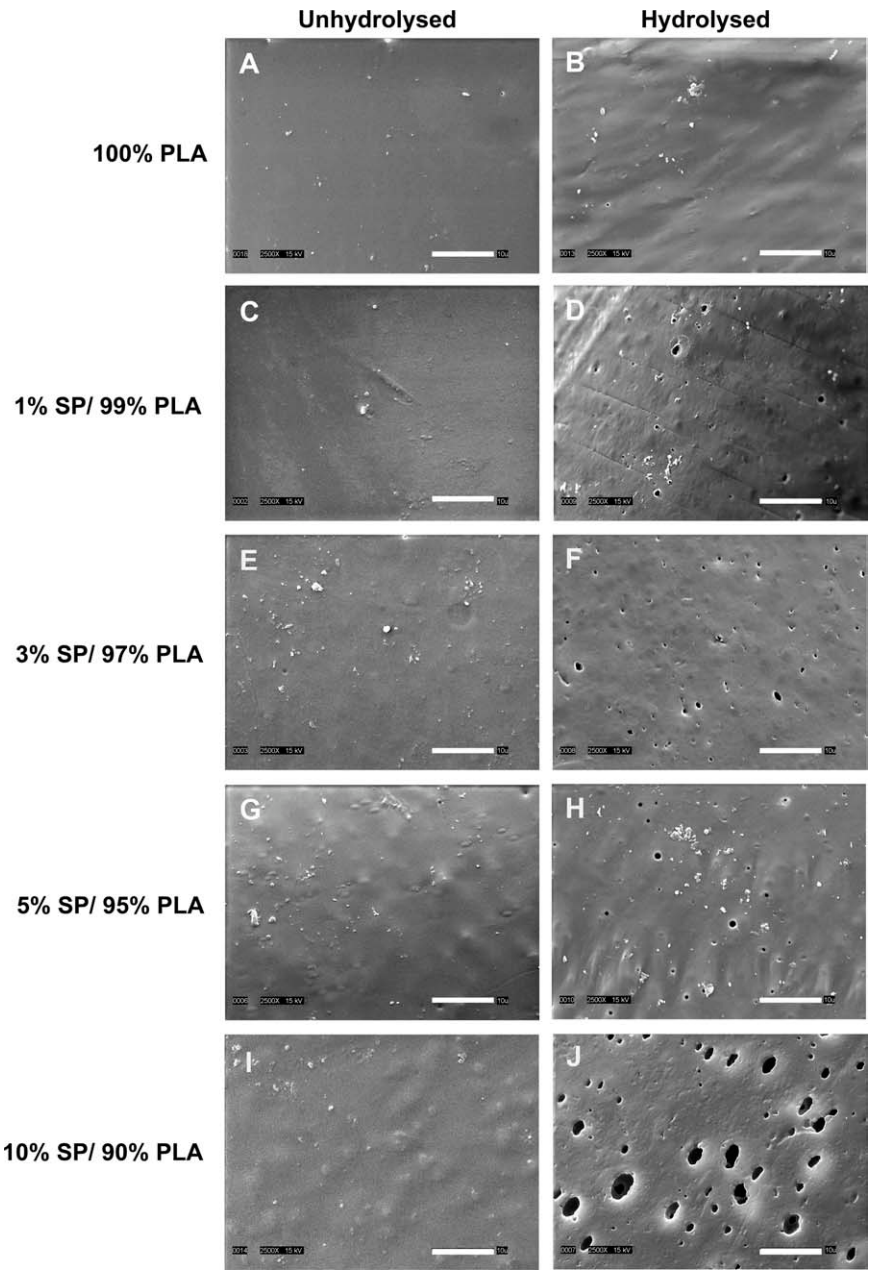

Figure 4 Scanning electron micrographs of unhydrolysed (A, C, E, G, and I) and hydrolysed (B, D, F, H, and J) 100% PLA and composite fibers. Scale bar: 10 μm, Magnification: 2500×.

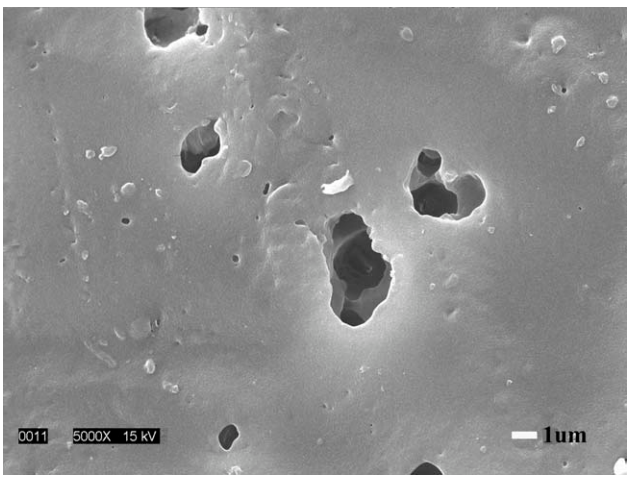

Figure 5 Scanning electron micrograph of hydrolysed 90% PLA/10% SP fiber acquired at a magnification of 5000× showing micropores that continue deep into the fiber.

1717 cm^{-1} [Fig. 8(A)]. The high intensity band at 1246 cm^{-1} could be assigned to —C— O stretching vibrations in complex in-plane ring ester modes[11,12] while the band at 1098 cm^{-1} could be assigned to symmetric C—C stretching vibrations of glycol groups [Fig. 8(A)].[11] The strong band at 726 cm^{-1} of 100% SP could be assigned to ring CH out of plane deformation. The bands observed in the 1430 – 1330 cm^{-1} range could be due to asymmetric SO_2 stretching from sulfonates in the SP polymer [Fig. 8(A)]. The FTIR band at 1717.7 cm^{-1}, which corresponds to C=O stretching[10] in the SP polymer was used to detect the localization of SP polymer in composite fiber cross sections [Fig. 8(A)]. Analysis of the intensity of 1717.7 cm^{-1} band using 2D contour maps and 3D maps (not shown) showed that SP was more randomly distributed throughout the composite fiber cross section in fibers with 10 [Figs. 9 and 11(A)], 5, and 3% SP (not shown) than those with 1% SP content [Figs. 10 and 11(B)]. Compared to 10, 5, and 3% SP fibers those with 99% PLA/1% SP had SP localized either at the center or at the edges of the fiber [Figs. 10 and 11(B)].

DISCUSSION

Three-dimensional scaffolds designed for tissue engineering applications require sufficient porosity to maintain continuous diffusion of culture media *in vitro* and/or blood *in vivo* into the scaffold for uniform cell growth and proliferation throughout the scaffold.[1] Although scaffolds fabricated using nonwoven structures provide a high degree of porosity in both the lateral and longitudinal direction of the structure, increased thickness of the scaffold reduces the degree of porosity and detrimentally affects diffusion of culture media or blood into the scaffold. Therefore, it is important to investigate methods to improve diffusional properties of polymeric scaffolds for tissue engineering applications.

Increase of liquid transfer properties along the longitudinal and lateral directions of a nonwoven structure can be accomplished by using two

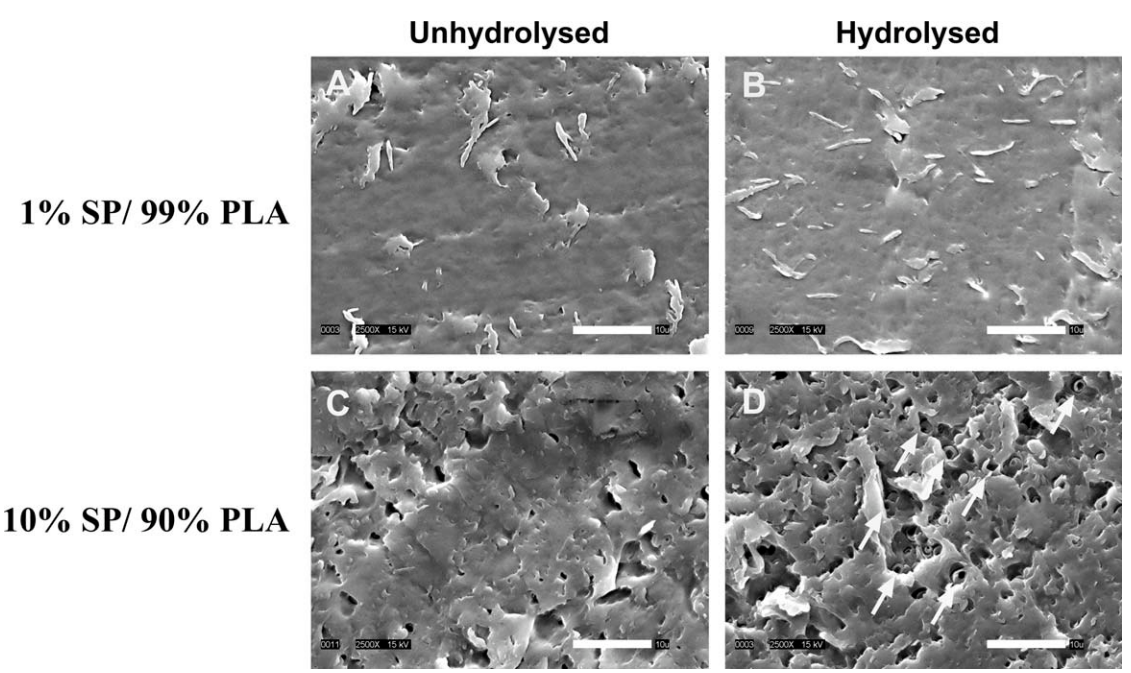

Figure 6 Scanning electron micrographs of 40 μm thin sections of unhydrolysed (A and C) and hydrolysed (B and D) composite fibers. (A, B) 99% PLA/1% SP and (C, D) 90% PLA/10% SP composite fibers. Micropores on hydrolysed fiber cross sections are indicated by arrows. Scale bar: 10 μm, Magnification: 2500×.

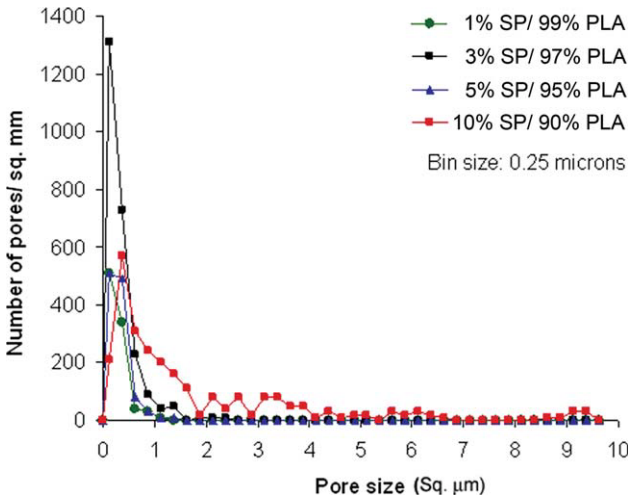

Figure 7 Pore size distribution of hydrolysed composite fibers. [Color figure can be viewed in the online issue, which is available at www.interscience.wiley.com.]

methods. The first is the use of microporous hollow fibers[13] to fabricate nonwoven structures. The hollow fibers would improve diffusion in the longitudinal direction of the structure while micropores on the hollow fiber walls would allow diffusion in the transverse direction of the structure. This configuration would significantly increase the final diffusional properties of the structure in both directions. The second method consists of generating micropores that run as channels inside the fibers with their pore openings on the surface of the fiber. These continuous micropores and channels in fibers would also increase diffusional properties in the longitudinal and transverse directions of the structure. The first stage of developing either microporous hollow fibers or fibers containing microchannels is to determine an appropriate method of creating random and well-distributed micropores on fiber surfaces.

In this study, we have investigated the use of a water-dispersible polymer combined with a more stable polymer to develop microporous fibers via a melt extrusion process. A water-dispersible polymer, SP, was blended at molten state with PLA and melt-extruded to produce filaments having 99% PLA/1% SP, 97% PLA/3% SP, 95% PLA/5% SP, and 90% PLA/10% SP compositions. This particular sulfonted copolyester was selected as the minor phase as it is readily dispersible using water at temperatures at which minimum or no degradation occurred to PLA. Additionally, the ability to use water as the dispersion medium with SP would be advantageous in creating biocompatible scaffolds for tissue engineering applications. Use of other dispersion media, such as solvents, acids, and alkali could leave residual chemicals in fibers causing toxic and harmful effects to cells cultured on resultant scaffolds. Previous studies have reported the use of dissolvable additives to form micropores in fibers. Dry silica or colloidal $CaCO_3$ has been added to create pores in copolyesters.[4] Chemical additives such as Na alkanesulfonate, Na magnesium dicarboxybenzene-sulfonate, and a mixture of polyethylene glycol and C12–13 alkanesulfonic acid sodium salt have also been reported to create pores when added to a copolyester.[4] Use of a water-dispersible secondary polymer to create micropores in a fiber has not been fully investigated. A secondary polymer having comparable thermal properties to the matrix polymer could be used to create micropores in the resultant fibers via melt spinning.[14,15] In such a binary polymer blend, the

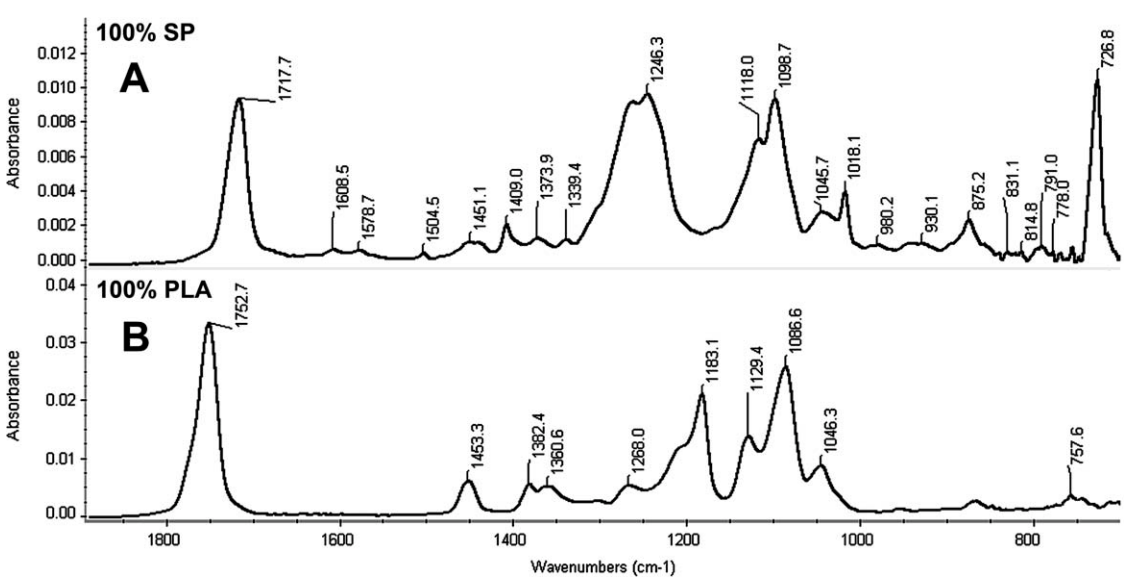

Figure 8 Fourier transform infrared spectra of (A) 100% sulfonated copolyester (SP) and (B) 100% poly(lactic acid) (PLA) polymers.

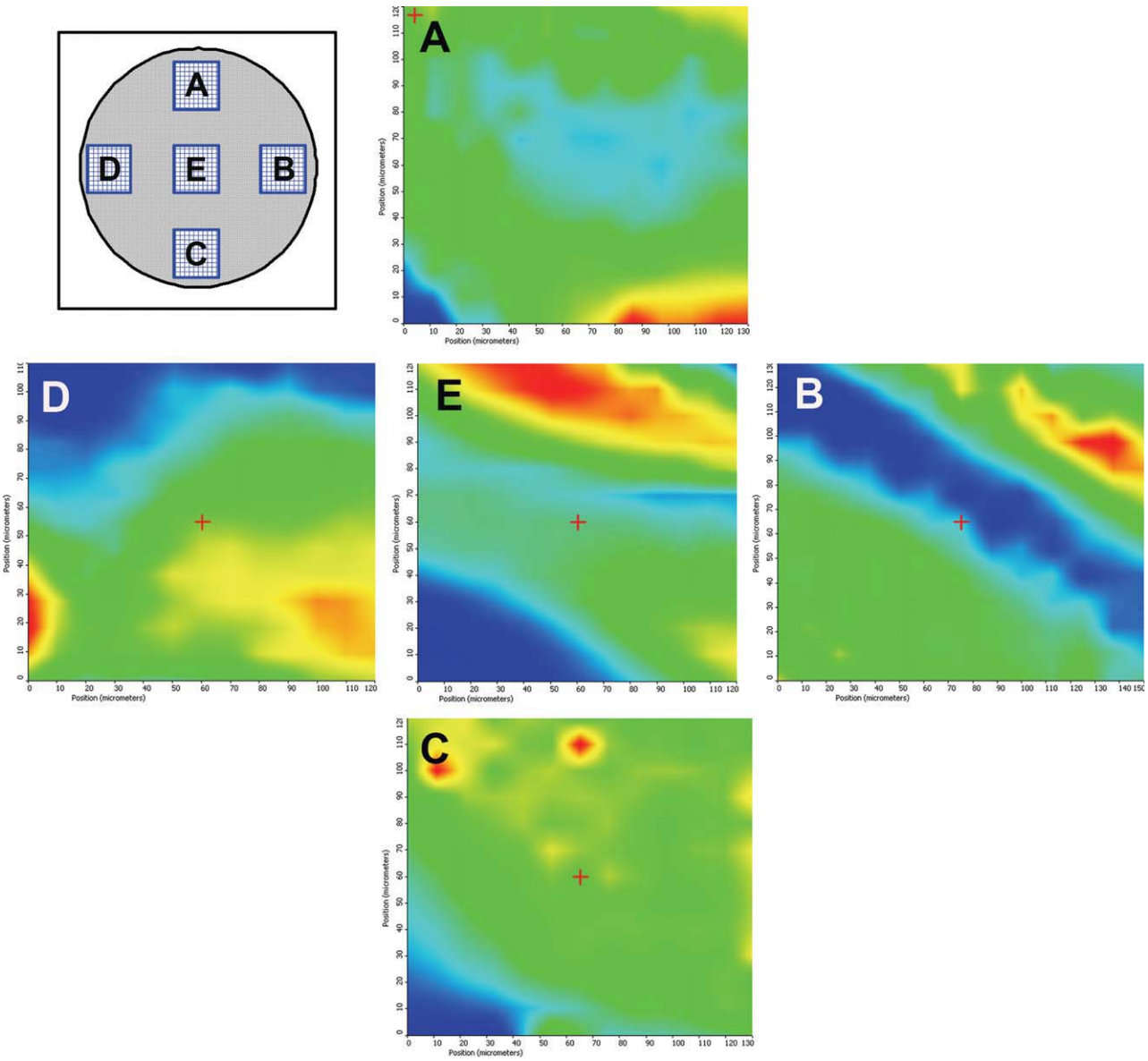

Figure 9 Contour maps showing the variation in peak height of 1717.7 cm^{-1} band indicative of localization of sulfonated copolyester (SP) in regions of an unhydrolysed 90% PLA/10% SP composite fiber cross section. Inset shows the corresponding areas mapped on the fiber cross section: (A) Top edge, (B) Right edge, (C) Bottom edge, (D) Left edge, and (E) Center of the fiber. The size of each area was 12.1 $\times$ 10^3 μm^2. Both horizontal and vertical axes shows the height and width of the scanned area from 0 to 13 μm. The intensity levels of 1717.7 cm^{-1} band in the contour maps varies from 0.5−0.65 (blue), 0.65–0.75 (turquoise), 0.75–0.95 (green), 0.95–1.05 (yellow), and 1.05–1.20 (red). [Color figure can be viewed in the online issue, which is available at www.interscience.wiley.com.]

morphology of the minor phase achieved during melt mixing would delineate the size and the arrangement of pores in the fiber. Previous studies have shown that the final morphology of the minor phase depends on: (1) viscosity or torque ratio, (2) composition, (3) shear stress, and (4) interfacial characteristics between the two polymers.[16]

Previous investigations have shown that the minor component is finely and uniformly distributed if it has a lower viscosity than the major component.[16] Avgeropolous et al.[17] and Karger-Kocsis et al.[18] reported that the particle size of the minor phase increased with viscosity ratio (calculated as torque ratio). Favis et al.[16] showed that the size of the minor phase was reduced below a torque ratio of 1 with a minimum particle size appearing at a torque ratio of 0.15. In this study, the torque ratio between 100% SP and 100% PLA remained below 1 during mixing in the micro compounder. This indicated that SP (minor component) was uniformly distributed in the PLA matrix during mixing and a fine particle size could be achieved by using the present

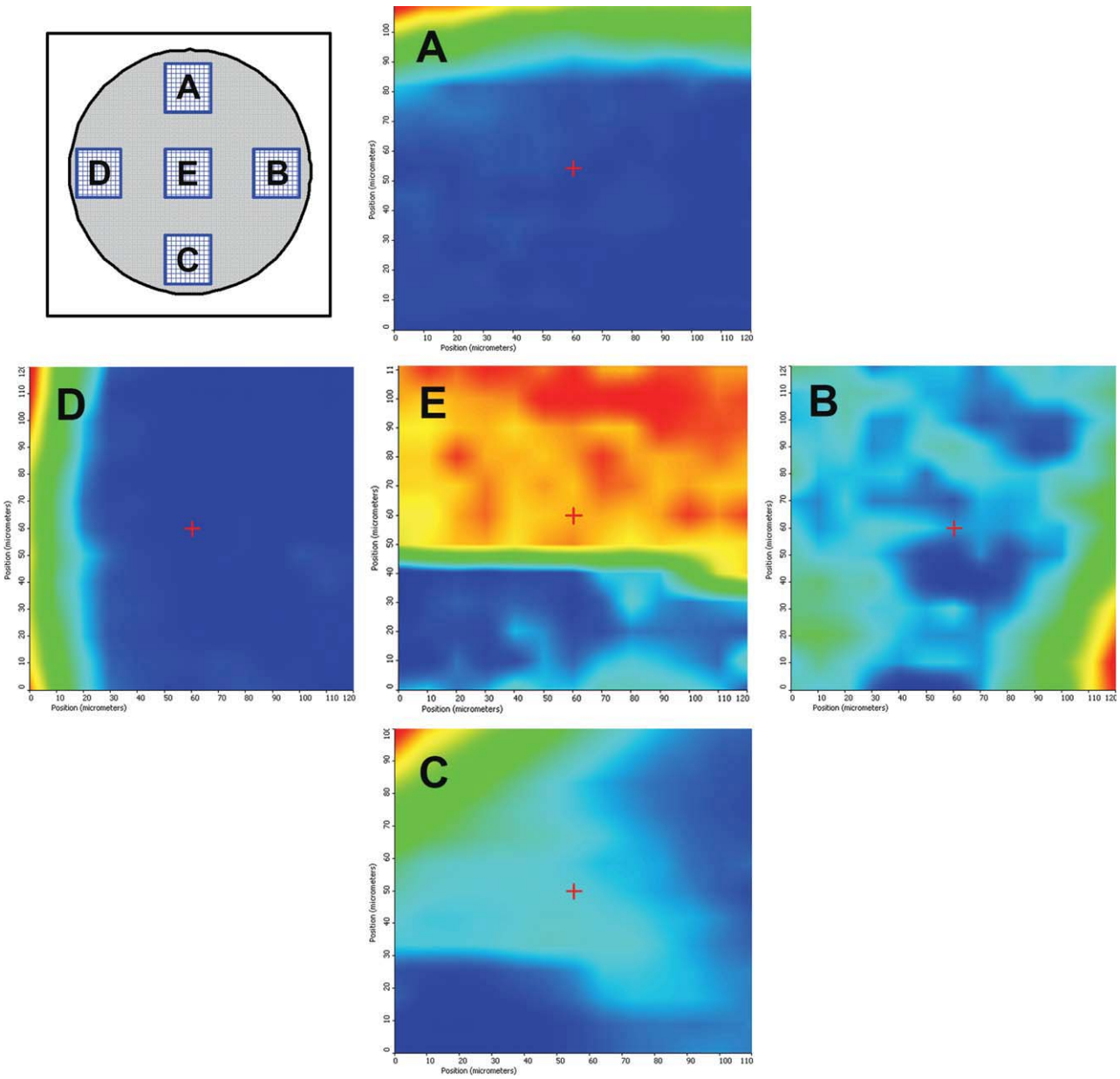

Figure 10 Contour maps of peak intensity at 1717.7 cm^{-1} indicative of localization of sulfonated copolyester (SP) in regions of an unhydrolysed 90% PLA/ 1% SP composite fiber cross section. Inset shows the corresponding areas mapped on the fiber cross section: (A) Top edge, (B) Right edge, (C) Bottom edge, (D) Left edge, and (E) Center of the fiber. The size of each area was 12.1 $\times$ 10^3 μm^2. Both horizontal and vertical axes shows the height and width of the scanned area from 0 to 13 μm. The intensity levels of 1717.7 cm^{-1} band in the contour maps varies from 0.5−0.65 (blue), 0.65–0.75 (turquoise), 0.75–0.95 (green), 0.95–1.05 (yellow), and 1.05–1.20 (red). [Color figure can be viewed in the online issue, which is available at www.interscience.wiley.com.]

processing protocol. The SP used in this study was highly water-dispersible allowing easy removal from the composite fiber.[19] The compatible thermal properties of SP and PLA created an intimate yet phase separated mixture to create a hybrid composite fiber. This random dispersion of SP in the PLA matrix resulted in well-distributed, discrete micropores in the fibers.

The glass transition temperature of both SP and PLA polymers decreased after melt extruding them into fibers. This indicated a microstructural change in both polymers during the extrusion process, which could have created more micro voids leading to increased chain mobility and thus a decrease in glass transition temperature. The glass transition temperature (T_g) of composite fibers was higher than that of 100% SP fibers but similar to that of 100% PLA polymer. The T_g of composite fibers behaved according to the T_g of a typical polymer blend with the measured values similar to calculated values by

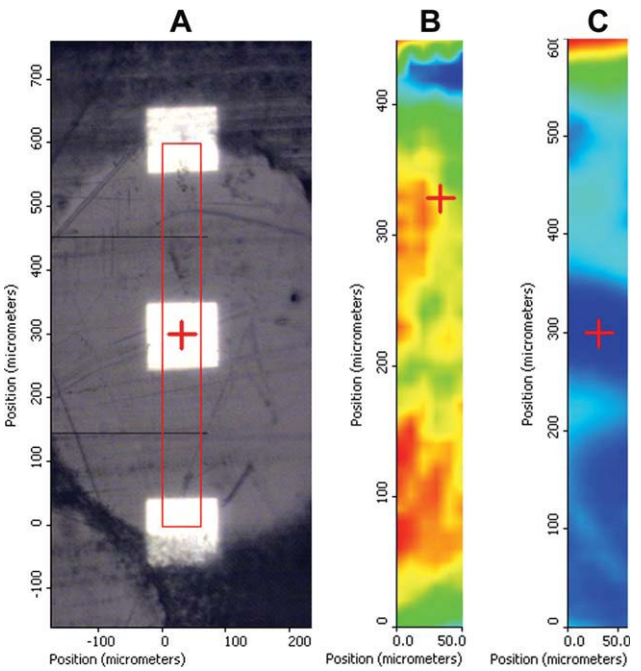

Figure 11 Variation in peak intensity of 1717.7 cm^{-1} band indicating sulfonated copolyester (SP) localization across the diameter of unhydrolysed composite fibers. (A) Video image of the mapped area; red grid within the bright circular fiber cross section shows a representation of the scanned area across a fiber diameter. The width of the area was 50 μm with length dependent on fiber diameter, (B) Contour map with intensity gradients of 1717.7 cm^{-1} band on an unhydrolysed 90% PLA/ 10% SP composite fiber, and (C) Contour map with intensity gradients of 1717.7 cm^{-1} band on an unhydrolysed 99% PLA/1% SP composite fiber. The intensity levels of 1717.7 cm^{-1} band in the contour maps varies from 0.5–0.65 (blue), 0.65–0.75 (turquoise), 0.75–0.95 (green), 0.95–1.05 (yellow), and 1.05–1.20 (red). [Color figure can be viewed in the online issue, which is available at www.interscience.wiley.com.]

the Fox equation ($1/T_g = w_1/T_1 + w_2/T_2$; w_1, w_2, and T_1, T_2 are weight fractions and pure component glass transitions of PLA and SP fibers, respectively).[20] The DSC thermograms of composite fibers showed a single glass transition temperature, especially at low SP contents, indicating a miscible blend between PLA and SP.[20,21] However, it is also possible that at low content of SP ($\leq$ 10%) in composite fibers, the glass transition of the composite fibers was not affected by SP. It has been shown that the T_g of pure components should differ by at least 20°C to resolve and distinguish them in thermograms.[20] This accounts for a minimum of 10 to 20 wt % of the minor component (SP) in the composite fiber. In this study, presence of a very weak transition at temperatures closer to T_g of SP fiber was observed in the DSC endotherms of 90% PLA/10% SP fibers indicating a partial miscibility of PLA and SP at 10% SP content in the composite fibers.[20]

Depression of the melting point during blending of crystalline with amorphous polymers has been reported by other authors.[22] However, in this study, a depression of the melting point was not observed, indicating that the SP content used in composite fibers was not sufficient to create a significant effect on melting. Unlike previous studies,[21] in this study there was no considerable change in the crystallization temperature of composite fibers compared to that of the extruded 100% PLA fibers. The melt endotherm of composite fibers consisted of a split peak, which indicated the presence of two types or sizes of crystals.[23,24] However, with the high crystallization exotherm that existed in DSC thermograms, these extruded composite fibers were observed to be amorphous. The extrusion process and minimum drawing of fibers after extrusion may have caused the extruded fibers to be amorphous. In addition, it has also been shown that crystalline lamellae have a tendency to thicken via partial melting and reorganize at the heating rates provided in the DSC experiment.[25] This phenomenon could be another reason to observe multiple melt endotherms in composite fibers in this study.

Scanning electron microscopy studies showed that it was possible to create micropores by hydrodispersing the SP component in the composite fibers using the protocol presented in this study. Both fiber surface and cross sections consisted of randomly distributed pores with varying sizes. The pore size distribution was dependent on the SP content in the composite fibers where larger pores were observed with 10% SP content than with others fibers with lower SP concentrations. It has been reported that in an immiscible polymer blend, a wide range of sizes and shapes could be obtained for the dispersed phase (minor phase) during processing.[26] These shapes that range from submicron to a hundred microns could be spherical, ellipsoidal, cylindrical, ribbonlike, cocontinuous, and subinclusion types.[26] A spherical dispersed phase of SP would result in a random distribution of pores on the fiber surface after hydrodispersion while a cocontinuous phase of SP would create continuous microchannels in the hydrodispersed fiber. In this study, SEM analysis showed the presence of micropores on both the fiber surface and fiber cross sections of hydrodispersed composite fibers. This indicated that the SP was dispersed in PLA matrix either in a spherical (droplet) or cocontinuous morphology. However, recent investigations on PE–PS blends have shown that a 50/50 polymer ratio for the blend is required to maintain a stable cocontinuous structure,[27] which instigate doubts on our observations of a cocontinuous morphology in PLA/SP blend. Porosity of the fibers can be measured to further characterize the porosity and interconnectivity of pores in resultant fibers. This

study showed that a significant number of pores in the fibers were below 4 μm^2. Liquid porosimetry could be used to measure the porosity of these fibers as the amount of pressure used in liquid porosimetry is lower compared to the pressure required for mercury intrusion porosimetry, thus preventing distortion of fibers during testing.[28,29]

Localization of SP in the PLA matrix was determined using FTIR mapping technique. FTIR mapping techniques were used to confirm the morphology of the PLA/SP blend and the results of the SEM analyses of the fiber cross sections. Compared to unhydrolysed 99% PLA/1% SP fibers, the locations where SP was highly concentrated were randomly distributed in 10% SP fibers. This was clearly indicated by the randomly distributed, high intensity areas of the 1717.7 cm^{-1} band in unhydrolyzed 90% PLA/10% SP fiber cross sections. The highly concentrated areas of SP in unhydrolyzed 99% PLA/1% SP fibers were located at either the core or perimeter of the composite fibers. This indicated that 1% SP content was not sufficient to obtain a randomly distributed minor phase in PLA and SP polymer blends. In addition, this explained the results of the SEM studies where 1% SP fibers only showed micropores on their fiber surfaces but not on their cross sections.

Hydrodispersion of SP from the composite fibers could alter the mechanical properties of the resultant fibers. Removal of one component to create micropores in composite fibers or fiber blends could reduce the tensile strength in the resultant fibers. This may be solely due to the fact that removal of one component reduces the amount of material in the fiber causing a weaker fiber. In addition, creation of void spaces in the fiber breaks the continuity of the material preventing uniform force distribution along the fiber, producing many weak points. To maintain sufficient strength and obtain optimal amount of porosity, a balance has to be achieved between the concentration of SP in fibers and the mechanical properties of the fiber. This ratio would also depend on the end use of the microporous fibers as some applications require more porous fibers, compromising strength. Further, a previous study on an immiscible two phase fiber blend using PLA and poly(butylene adipate-*co*-terephthalate) (PBAT) has shown decreased tensile strength and modulus, and increased elongation and toughness with no effect on the final degree of crystallinity.[14] This further indicates that a balance must be achieved in the spinning conditions and end use of the PLA/SP fibers. The relationship of factors, such as tensile strength, modulus, and porosity before and after hydrodispersion of SP in the PLA/SP blend would be investigated in future studies.

Although micropores were clearly visible on the fiber surfaces and cross sections, the distribution of the pores on the fibers was not quantified in this study. This presents one of the limitations of this study and would be addressed in future studies. Another limitation of this study is the absence of a relationship between the SP content in the fiber and the distribution of micropores in the fiber cross sections. Generation of such as relationship based on intensive FTIR mapping will be undertaken in our future studies. In addition, measurement of fluid diffusion across hydrodispersed porous fibers in comparison to non-porous melt spun fibers would clearly indicate the increase in diffusional properties of these fibers. Increased diffusional rates through a single fiber, fiber bundles, or fibrous scaffolds fabricated using resultant porous fibers would delineate the potential use of these fibers as a scaffold for tissue engineering applications.

In summary, we have investigated the use of SP as a minor phase and PLA as a major phase in a multiphase polymer blend to create micropores in melt-extruded PLA/SP composite fibers. Thermal analysis using DSC showed that partial miscibility could be obtained between PLA and SP polymers using the extrusion protocol used in this study. Random dispersion of SP throughout PLA/SP fiber cross sections was evident. This random distribution of SP was more prominent in fibers with 3, 5, and 10% SP than fibers with 1% SP. The micropores observed on both fiber surfaces and fiber cross sections of 3, 5, and 10% SP fibers indicated that SP was dispersed in PLA as either droplet or cocontinuous phase morphology. The size of micropores was affected by the SP content in composite fibers.

These results show that micropores can be successfully created in fibers by using a blend of SP and PLA and hydrodispersing SP from the resultant fibers. This technology can be used to create microporous hollow fibers or fibers with microchannels. Nonwoven scaffolds fabricated by using these fibers for tissue engineering applications would have increased diffusional properties, potentially promoting uniform cell growth throughout the scaffold both *in vitro* and *in vivo*.

The authors wish to thank Dr. Svetlana Verenich, Birgit Andersen, Seth McCullen, Mehdi Afshari & Marcus Hunt for their technical assistance.

References

1. Chen, G.; Ushida, T.; Tateishi, T. Macromol Biosci 2002, 2, 67.
2. Chapekar, M. S. J Biomed Mater Res 2000, 53, 617.
3. Godbey, W. T.; Atala, A. Ann N Y Acad Sci 2002, 961, 10.
4. Beyreuther, R.; Schauer, G. Sci Technol 2000, 299–353.
5. Kim, J. J. J Membr Sci 1995, 108, 25.
6. Thakur, K. A. M. Macromolecules 1996, 29, 8844.
7. Elenga, R.; Seguela, R.; Rietsch, F. Polymer 1991, 32, 1975.
8. Barbanti, S. H.; Santos, A. R., Jr.; Zavaglia, C. A.; Duek, E. A. J Mater Sci Mater Med 2004, 15, 1315.

9. Zhang, J. F.; Sun, X. Polym Int 2004, 53, 716.
10. Catiker, E.; Gumusderelioglu, M.; Guner, A. Polym Int 2000, 49, 728.
11. Miyake, A. J Polym Sci 1959, 38, 479.
12. Cole, K. C.; Ajji, A.; Pellerin, E. Macromolecules 2002, 35, 770.
13. Rovere, A.; Shambaugh, R. L. Ind Eng Chem Res 2001, 40, 176.
14. Jian, L.; Wolcott, M.; Zhang, J. Biomacromolecules 2006, 7, 199.
15. Sarazin, P.; Favis, B. D. Biomacromolecules 2003, 4, 1669.
16. Favis, B. D.; Chalifoux, J. P. Polym Eng Sci 1987, 27, 1591.
17. Avgerpoulos, G. N.; Weissert, F. C.; Biddison, P. H.; Bohm, G. C. A. Rubber Chem Technol 1976, 49, 93.
18. Karger-Kocsis, J.; Kallo, A.; Kuleznev, V. N. Polymer 1984, 25, 279.
19. Collyer, S. D.; Bradbury, S. E.; Hatfield, J. V.; Higson, S. P. J. Electroanalysis 2000, 13, 332.
20. Kalika, D. S. Viscoelastic Characterization of Polymer Blends; John Wiley: New York, 2000.
21. Shonaike, G. O. Miscibility of Nylon 66/Santoprene Blends; Mercel Dekker: New York, 1999.
22. Greco, R.; Mancarella, M.; Martuscelli, E.; Ragosta, G.; Jinghua, Y. Polymer 1929, 28, 1987.
23. Collins, M. J.; Zeronian, S. H.; Semmelmeyer, M. J Appl Polym Sci 1991, 42, 2149.
24. Skoog, D. A.; Holler, F. J.; Nieman, T. A. Principles of Instrumental Analysis; Hartcourt Brace College Pub: Orlando, FL, 1998.
25. Runt, J. P. Crystalline Polymer Blends; John Wiley: New York, 2000.
26. Favis, B. D. Factors Influencing the Morphology of Immiscible Polymer Blends in Melt Processing; John Wiley: New York, 2000.
27. Mekhilef, N.; Favis, B. D.; Carreau, P. J. J polym Sci Part B: Polym Phys 1997, 35, 293.
28. Miller, B.; Tyomkin, I. J Colloid Interface Sci 1994, 162, 163.
29. Hsieh, Y. Text Res J 1995, 65, 299.